

Multiply Stranded and Multiply Encircled Pseudorotaxanes[†]Peter R. Ashton,[‡] Matthew C. T. Fyfe,[‡] Peter T. Glink,[‡] Stephan Menzer,[§] J. Fraser Stoddart,^{*,‡,||} Andrew J. P. White,[§] and David J. Williams[§]

Contribution from The School of Chemistry, The University of Birmingham, Edgbaston, Birmingham B15 2TT, UK, and The Chemical Crystallography Laboratory, Department of Chemistry, Imperial College, South Kensington, London SW7 2AY, UK

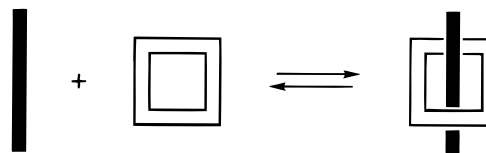
Received May 7, 1997. Revised Manuscript Received October 16, 1997[⊗]

Abstract: The self-assembly of four multicomponent rotaxane-like complexes, in which either (a) three or four dibenzo[24]crown-8 rings encircle threadlike oligoammonium cations $[\text{PhCH}_2(\text{NH}_2^+\text{CH}_2\text{C}_6\text{H}_4\text{CH}_2)_n\text{NH}_2^+\text{CH}_2\text{Ph}]$ ($n = 2$ or 3) to form multiply encircled pseudorotaxanes, or (b) three or four dibenzylammonium ions are threaded simultaneously through large macrocyclic polyethers, *viz.*, tris-*p*-phenylene[51]crown-15 and tetrakis-*p*-phenylene[68]crown-20, to give multiply stranded pseudorotaxanes, is described. These supramolecular entities are created on account of stabilizing $[\text{N}^+\text{H}\cdots\text{O}]$ and $[\text{C}\text{--}\text{H}\cdots\text{O}]$ hydrogen bonds, supplemented occasionally by aromatic face-to-face and edge-to-face interactions, and $[\text{C}\text{--}\text{H}\cdots\text{F}]$ intermolecular bonds. Evidence for the existence of these diverse pseudorotaxane architectures in solution, in the solid state, and in some cases, in the “gas phase”, is provided by ¹H NMR spectroscopy, X-ray crystallography, and mass spectrometry, respectively.

Introduction

One of the major areas of investigation in modern synthetic chemistry is the construction¹ of thermodynamically stable supramolecular² aggregates and arrays in a controlled and predictable manner utilizing self-assembly processes³ that rely upon noncovalent bonding interactions.⁴ One particularly interesting class of supramolecular aggregates is the so-called pseudorotaxanes.⁵ These supramolecular entities are comprised (Scheme 1) of one (or more) threadlike component(s) which is (are) encircled by one (or more) beadlike component(s). They are promising prototypes for a variety of nanoscopic machinelike systems,⁶ such as switches⁷ and shuttles.⁸ Until recently,

Scheme 1. A Generic [2]Pseudorotaxane, Created When a Macrocyclic Beadlike Component (open square) Encircles a Threadlike Component (black bar)^a



^a The prefix of an $[n]$ pseudorotaxane indicates that the complex is comprised of n components.

pseudorotaxanes have been prepared most conveniently by utilizing one of the following systems: (a) the van der Waals interactions⁹ between cyclodextrin derivatives and hydrophobic guests, (b) the metal–ligand interactions¹⁰ between metal ions, such as copper(I), and bipyridine-derived beads/threads, and (c) the attraction between π -electron-rich¹¹ (or π -electron-deficient¹²) macrocyclic hosts and π -electron-deficient (or π -electron-rich) threadlike guests. In the past few years, we have developed^{13–16} extremely simple self-assembling systems which produce pseudorotaxane complexes. They are based upon the association between secondary dialkylammonium ions, such as the linear threadlike cationic salts, dibenzylammonium

[†] Molecular Meccano, Part 24. For Part 23, see: Ashton, P. R.; Boyd, S. E.; Menzer, S.; Pasini, D.; Raymo, F. M.; Spencer, N.; Stoddart, J. F.; White, A. J. P.; Williams, D. J.; Wyatt, P. G. *J. Am. Chem. Soc.*, in press.

[‡] University of Birmingham.

[§] Imperial College.

^{||} Address for correspondence: Department of Chemistry and Biochemistry, University of California at Los Angeles, 405 Hilgard Avenue, Los Angeles, CA 90095.

[⊗] Abstract published in *Advance ACS Abstracts*, December 15, 1997.

(1) Fyfe, M. C. T.; Stoddart, J. F. *Acc. Chem. Res.* 1997, 30, 393–401.

(2) Lehn, J.-M. *Supramolecular Chemistry—Concepts and Perspectives*; VCH: Weinheim, 1995.

(3) Philp, D.; Stoddart, J. F. *Angew. Chem., Int. Ed. Engl.* 1996, 35, 1154–1196.

(4) Some recent examples serve to highlight the kinds of approaches being taken. See: (a) Fujita, M.; Ogura, D.; Miyazawa, M.; Oka, H.; Yamaguchi, K.; Ogura, K. *Nature (London)* 1995, 378, 469–471. (b) Hartgerink, J. D.; Granja, J. R.; Milligan, R. A.; Ghadiri, M. R. *J. Am. Chem. Soc.* 1996, 118, 43–50. (c) Zimmerman, S. C.; Zeng, F.; Reichert, D. E. C.; Kolotuchin, S. V. *Science* 1996, 271, 1095–1098. (d) Funeriu, D. P.; Lehn, J.-M.; Baum, G.; Fenske, D. *Chem. Eur. J.* 1997, 3, 99–104. (e) Meissner, R.; Garcias, X.; Mecozzi, S.; Rebek, J., Jr. *J. Am. Chem. Soc.* 1997, 119, 77–85. (f) Whang, D.; Kim, K. *J. Am. Chem. Soc.* 1997, 119, 451–452.

(5) Amabilino, D. B.; Anelli, P.-L.; Ashton, P. R.; Brown, G. R.; Córdova, E.; Godínez, L. A.; Hayes, W.; Kaifer, A. E.; Philp, D.; Slawin, A. M. Z.; Spencer, N.; Stoddart, J. F.; Tolley, M. S.; Williams, D. J. *J. Am. Chem. Soc.* 1995, 117, 11142–11170.

(6) For leading references, see: Credi, A.; Balzani, V.; Langford, S. J.; Stoddart, J. F. *J. Am. Chem. Soc.* 1997, 119, 2679–2681.

(7) Córdova, E.; Bissell, R. A.; Kaifer, A. E.; Stoddart, J. F. *Nature (London)* 1994, 369, 133–137.

(8) Anelli, P.-L.; Asakawa, M.; Ashton, P. R.; Bissell, R. A.; Clavier, G.; Górski, R.; Kaifer, A. E.; Langford, S. J.; Mattersteig, G.; Menzer, S.; Philp, D.; Slawin, A. M. Z.; Spencer, N.; Stoddart, J. F.; Tolley, M. S.; Williams, D. J. *Chem. Eur. J.* 1997, 3, 1113–1135.

(9) Wenz, G. *Angew. Chem., Int. Ed. Engl.* 1994, 33, 803–822.

(10) Baxter, P. N. W.; Sleiman, H.; Lehn, J.-M.; Rissanen, K. *Angew. Chem., Int. Ed. Engl.* 1997, 36, 1294–1296.

(11) For instance, see: Ashton, P. R.; Ballardini, R.; Balzani, V.; Belohradsky, M.; Gandolfi, M. T.; Philp, D.; Prodi, L.; Raymo, F. M.; Reddington, M. V.; Spencer, N.; Stoddart, J. F.; Venturi, M.; Williams, D. J. *J. Am. Chem. Soc.* 1996, 118, 4931–4951.

(12) For leading references, see: Asakawa, M.; Ashton, P. R.; Brown, G. R.; Hayes, W.; Menzer, S.; Stoddart, J. F.; White, A. J. P.; Williams, D. J. *Adv. Mater.* 1996, 8, 37–41.

(13) Ashton, P. R.; Chrystal, E. J. T.; Glink, P. T.; Menzer, S.; Schiavo, C.; Spencer, N.; Stoddart, J. F.; Tasker, P. A.; White, A. J. P.; Williams, D. J. *Chem. Eur. J.* 1996, 2, 709–728.

(14) Ashton, P. R.; Glink, P. T.; Stoddart, J. F.; Tasker, P. A.; White, A. J. P.; Williams, D. J. *Chem. Eur. J.* 1996, 2, 729–736.

(15) Ashton, P. R.; Collins, A. N.; Fyfe, M. C. T.; Glink, P. T.; Menzer, S.; Stoddart, J. F.; Williams, D. J. *Angew. Chem., Int. Ed. Engl.* 1997, 36, 59–62.

(16) Ashton, P. R.; Glink, P. T.; Martínez-Díaz, M.-V.; Stoddart, J. F.; White, A. J. P.; Williams, D. J. *Angew. Chem., Int. Ed. Engl.* 1996, 35, 1930–1933.

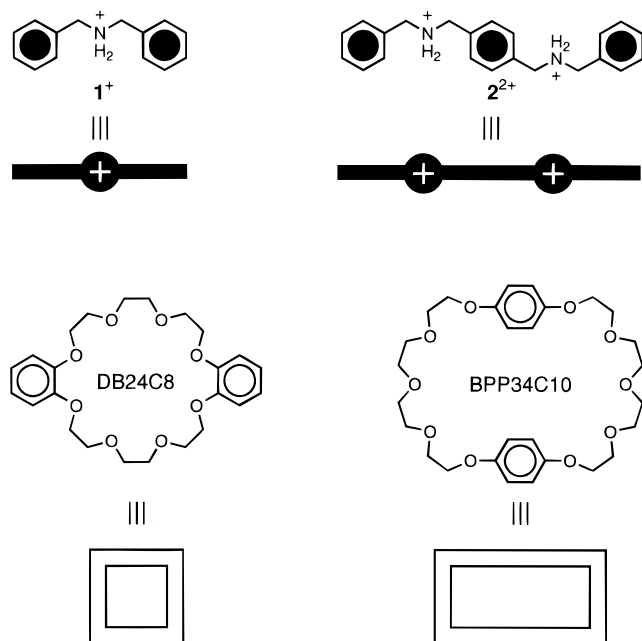
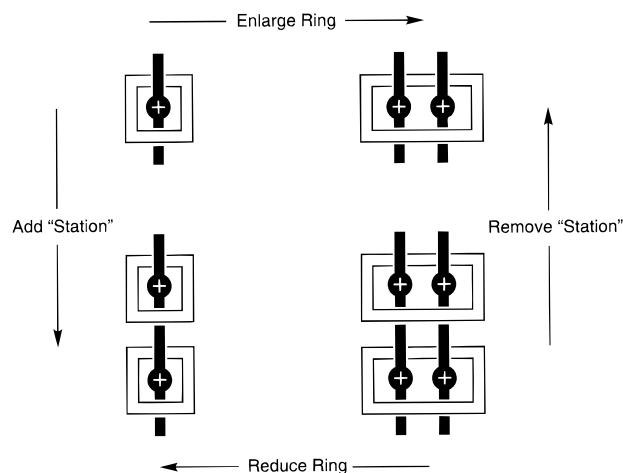


Figure 1. Chemical formulas and cartoon representations for the threadlike oligocations 1^+ and 2^{2+} (black bars) and the crown ethers DB24C8 (open squares) and BPP34C10 (open rectangles).

Scheme 2. Cartoon Representations Illustrating the Geometries and Stoichiometries of the Complexes between Linear Secondary Dialkylammonium Mono- and Dications (black bars) and Macrocyclic Polyethers (open squares and rectangles) Reported to Date



hexafluorophosphate ($1 \cdot \text{PF}_6$) and α, α' -bis(benzylammonium)-*p*-xylene bis(hexafluorophosphate) ($2 \cdot 2\text{PF}_6$) (Figure 1), and macrocyclic polyethers, such as dibenzo[24]crown-8 (DB24C8) and bis-*p*-phenylene[34]crown-10 (BPP34C10) (Figure 1), that have sufficiently large rings to permit the passage of alkyl and aryl groups through their cavities. These rotaxane-like superstructures, stabilized primarily by $[\text{N}^+ \cdots \text{H} \cdots \text{O}]$ and $[\text{C} \cdots \text{H} \cdots \text{O}]$ hydrogen bonds, provide a practicable and versatile recognition motif for supramolecular synthesis, in that the stoichiometries and geometries of complexation may be altered by changing either (a) the number of dialkylammonium centers in the cationic threadlike units, or (b) the size of the macrocyclic polyether's cavity.¹³ By way of illustration, we have reported¹⁷ to date, the characterization¹³ of four different types of pseudorotaxane complexes (Scheme 2) with stoichiometries (host:guest)

(17) For the synthesis of an alternative family of rotaxanes that are stabilized primarily by hydrogen bonding, see: Vögtle, F.; Dünwald, T.; Schmidt, T. *Acc. Chem. Res.* **1996**, *29*, 451–460 and references cited therein.

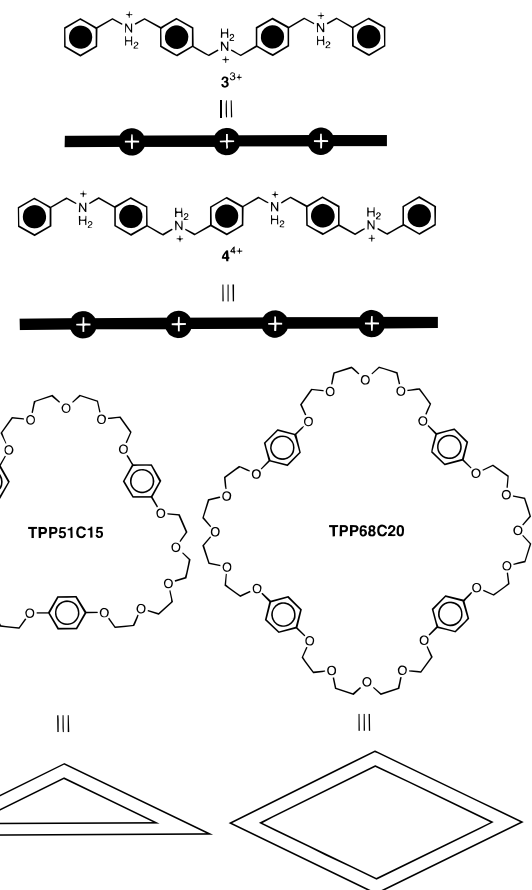
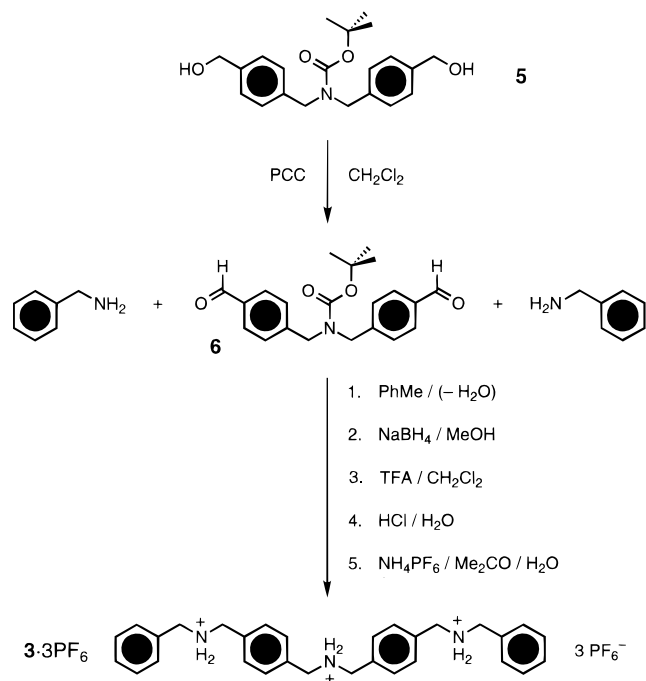


Figure 2. Chemical formulas and cartoon representations of the oligocations 3^{3+} and 4^{4+} (black bars) and the macrocyclic polyethers TPP51C15 (open triangle) and TPP68C20 (open diamond).

of 1:1 (e.g., $[\text{DB24C8} \cdot 1]^+$), 1:2 (e.g., $[\text{BPP34C10} \cdot (1)_2]^{2+}$), 2:1 (e.g., $[(\text{DB24C8})_2 \cdot 2]^{2+}$), and 2:2 (e.g., $[(\text{BPP34C10})_2 \cdot (2)_2]^{4+}$), respectively. These examples divulge that DB24C8 will accommodate only one secondary dialkylammonium center within its cavity to generate single-stranded pseudorotaxanes (e.g., $[\text{DB24C8} \cdot 1]^+$ and $[(\text{DB24C8})_2 \cdot 2]^{2+}$), while BPP34C10 can accommodate two such units to form double-stranded pseudorotaxane complexes (e.g., $[\text{BPP34C10} \cdot (1)_2]^{2+}$ and $[(\text{BPP34C10})_2 \cdot (2)_2]^{4+}$), and that separating the NH_2^+ centers of threadlike units by *p*-xylyl spacer groups allows each of these centers to be encircled by an individual crown ether (e.g., $[(\text{DB24C8})_2 \cdot 2]^{2+}$ and $[(\text{BPP34C10})_2 \cdot (2)_2]^{4+}$).¹³ We were thus intrigued to find out whether we could (a) add more NH_2^+ centers to the threadlike oligocations, in order to encircle more than two crown ethers around the threads, and (b) further increase the size of the crown ether macrocyclic cavity to see if more than two dialkylammonium ions could thread through even larger macrocyclic cavities. That is, can we extend the cartoon displayed in Scheme 2, both in a “north–south” and an “east–west” direction? Here, we report that multiply stranded and multiply encircled pseudorotaxane complexes are indeed capable of being formed and characterized, in solution, in the solid state, and in some instances, in the “gas phase”.

Results and Discussion

Supramolecular Strategy. In the knowledge that $2 \cdot 2\text{PF}_6$ forms a 2:1 complex (host:guest) with DB24C8, the obvious choices for tri- and tetracationic threadlike salts—that might be capable of complexing with three and four crown ethers, respectively—are those in which the NH_2^+ centers are evenly spaced using *p*-xylyl groups, i.e., as in the salts $3 \cdot 3\text{PF}_6$ and

Scheme 3. Synthesis of the Tricationic Salt **3**·**3PF₆**

4·**4PF₆** (Figure 2). As host molecules, suitable for including more than two dialkylammonium cations within their cavities, we chose to study the crown ethers tris-*p*-phenylene[51]crown-15 (TPP51C15) and tetrakis-*p*-phenylene[68]crown-20 (TPP68C20) (Figure 2), *i.e.*, higher homologues of the crown ether BPP34C10. These two “new” crown ethers, prepared previously to act as templates for the formation of multiply interlocked ring systems, *i.e.*, catenanes,¹⁸ might be expected to thread three and four thread-like cations through their individual cavities, primarily as a result of [N⁺—H···O] hydrogen-bonding interactions with their respective three and four tetraethylene glycol-derived polyether loops.

Synthesis. The tricationic salt **3**·**3PF₆** was obtained in an overall yield of 39% (Scheme 3) via a six-step process from the known¹⁴ diol **5**. The tetracationic salt **4**·**4PF₆** was prepared (Scheme 4) in 40% overall yield from benzylamine and methyl 4-formylbenzoate using a similar protocol. The macrocyclic polyethers TPP51C15 and TPP68C20 were synthesized according to established procedures.¹⁸

Complexation: Tricationic Salt **3·**3PF₆** and DB24C8.** Although the tricationic salt **3**·**3PF₆** is soluble in polar solvents, such as Me₂CO and MeCN, that are capable of hydrogen bonding with the NH₂⁺ centers, not surprisingly, it is insoluble¹⁹ in halogenated solvents such as CH₂Cl₂ and CHCl₃. A solution of the salt in either MeCN or Me₂CO in the presence of >3 mol equiv of DB24C8 may be diluted with CH₂Cl₂ or CHCl₃ such that no precipitate is formed from what is essentially a solution of **3**·**3PF₆** and DB24C8 in the halogenated solvent. This behavior, comparable with solubility characteristics we have observed¹³ for the dicationic salt **2**·**2PF₆** previously, points to the formation of a multiply encircled complex that is soluble in chlorinated solvents.

Analysis of an CD₃CN solution containing a 3:1 molar ratio of DB24C8 and **3**·**3PF₆** revealed a complicated scenario, since

(18) Amabilino, D. B.; Ashton, P. R.; Brown, C. L.; Córdova, E.; Gódinez, L. A.; Goodnow, T. T.; Kaifer, A. E.; Newton, S. P.; Pietraszkiewicz, M.; Philp, D.; Raymo, F. M.; Reder, A. S.; Rutland, M. T.; Slawin, A. M. Z.; Spencer, N.; Stoddart, J. F.; Vicent, C.; Williams, D. J. *J. Am. Chem. Soc.* **1995**, *117*, 1271–1293.

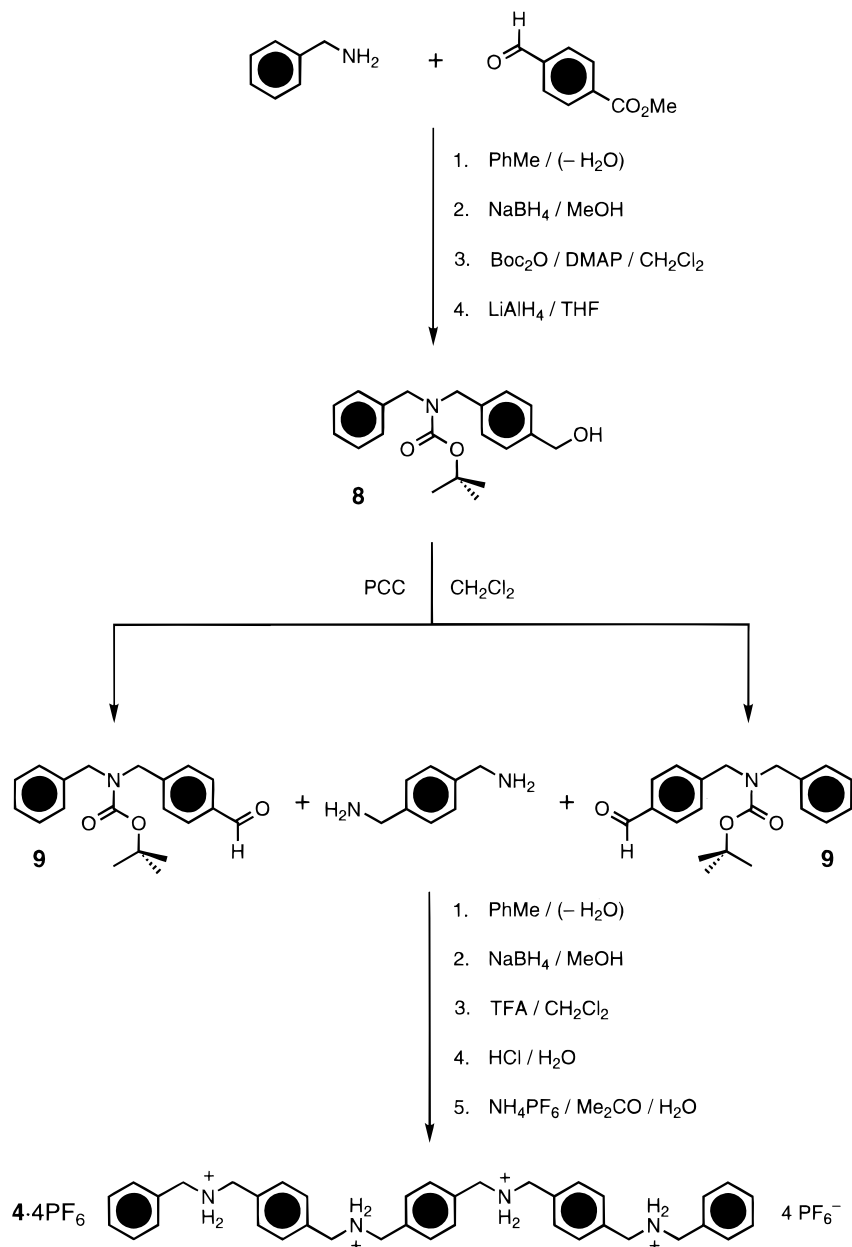
(19) We have noted previously¹³ that the hexafluorophosphate salts of **1**⁺ and of **2**²⁺ are practically insoluble in CHCl₃ and CH₂Cl₂ in the absence of a suitably sized crown ether for complexation.

the supramolecular system is characterized by equilibria involving slow kinetic exchange on the ¹H NMR time scale at 300 MHz as a result of the large (but surmountable) steric barrier for the slippage of the rather small DB24C8 ring over the relatively bulky phenyl and *p*-xylyl units. Signals associated with the uncomplexed crown ether and the “free” tricationic salt, besides those for the 1:1, 2:1, and 3:1 complexes formed between the two species, are present. The complexity of the ¹H NMR spectrum makes signal assignment for the individual complexes rather difficult. In the case of complexation between **3**·**3PF₆** and DB24C8 (Scheme 5), there are two possible “isomeric” 1:1 complexes [DB24C8·**3**]³⁺ (**A** and **B**), two “isomeric” 2:1 complexes [(DB24C8)₂·**3**]³⁺ (**C** and **D**), and one 3:1 complex [(DB24C8)₃·**3**]³⁺. In addition to uncomplexed host and guest species, this situation means that there are a total of 13 different environments for the protons of the α-, β-, and γ-OCH₂ units of the crown ether in the slowly equilibrating mixture. Additionally, the necessity of using polar solvents, such as CD₃CN or CD₃COCD₃, to dissolve the tricationic salt means that association constants¹³ for the individual DB24C8·R₂NH₂⁺ complexes are in the region of 10²–10³ M⁻¹, an order of magnitude which corresponds to a significant amount of each of these species existing in solution at the concentrations usually employed for recording ¹H NMR spectra. We have found that the complex spectroscopic behavior can be minimized by obtaining the ¹H NMR spectrum of **3**·**3PF₆** in the presence of an excess (~10 mol equiv) of DB24C8 in a CDCl₃/CD₃CN solvent mixture. The presence of the halogenated solvent increases the association constants for the complexation processes, while the excess of the crown ether ensures that the equilibria between the uncomplexed and rotaxane-like systems are driven toward the 3:1 complex. In this case, a spectrum was obtained²⁰ in which two major species, *viz.*, the excess of uncomplexed DB24C8 and the [4]pseudorotaxane, [(DB24C8)₃·**3**]³⁺, were found to be present in solution. The stoichiometry of the complex was ascertained to be 3:1 from an examination of the relative intensities of the signals associated with the complexed host and guest for the (a) aromatic protons and (b) methylene protons.

Crystals were obtained when *i*-Pr₂O vapor was allowed to diffuse into an Me₂CO solution containing a 3:1 molar mixture of DB24C8 and **3**·**3PF₆**. Analysis of one such crystal by liquid secondary ion mass spectrometry (LSIMS) revealed²⁰ an intense peak at *m/z* 2077, corresponding to the 3:1 complex with the loss of only one of its counterions, *i.e.*, [(DB24C8)₃·**3**·**2PF₆**]⁺. The fact that the integrity of the 3:1 complex is maintained in the “gas phase”, with an intensity *ca.* 3% of that of the base peak (in this case, the 1:1 complex [DB24C8·**3** – 2H⁺] which is observed at *m/z* 884), is a testament to the stability, and presumably the slow rates of dissociation (*cf.*, the solution state), of the four-component pseudorotaxane superstructure.

A single crystal of the complex was analyzed by X-ray crystallography. The solid-state structure of the 3:1 complex [(DB24C8)₃·**3**][PF₆]₃ shows (Figure 3) the trication to be threaded through the centers of three DB24C8 macrocycles, one of which (**A**) has a folded geometry, while the others (**B** and **C**) have extended C_i-like conformations. Host–guest stabilization is achieved by a combination of [N⁺—H···O] and [C—H···O] hydrogen bonding, supplemented by face-to-face π–π stacking between the *p*-xylyl rings of the trication and one of the catechol rings of each of the DB24C8 hosts (Figure 4). Inspection of the packing of the [4]pseudorotaxanes reveals (Figure 5) that centrosymmetrically related pairs are oriented such that one of the terminal phenyl rings of one trication (that proximal to

(20) See the Supporting Information for details.

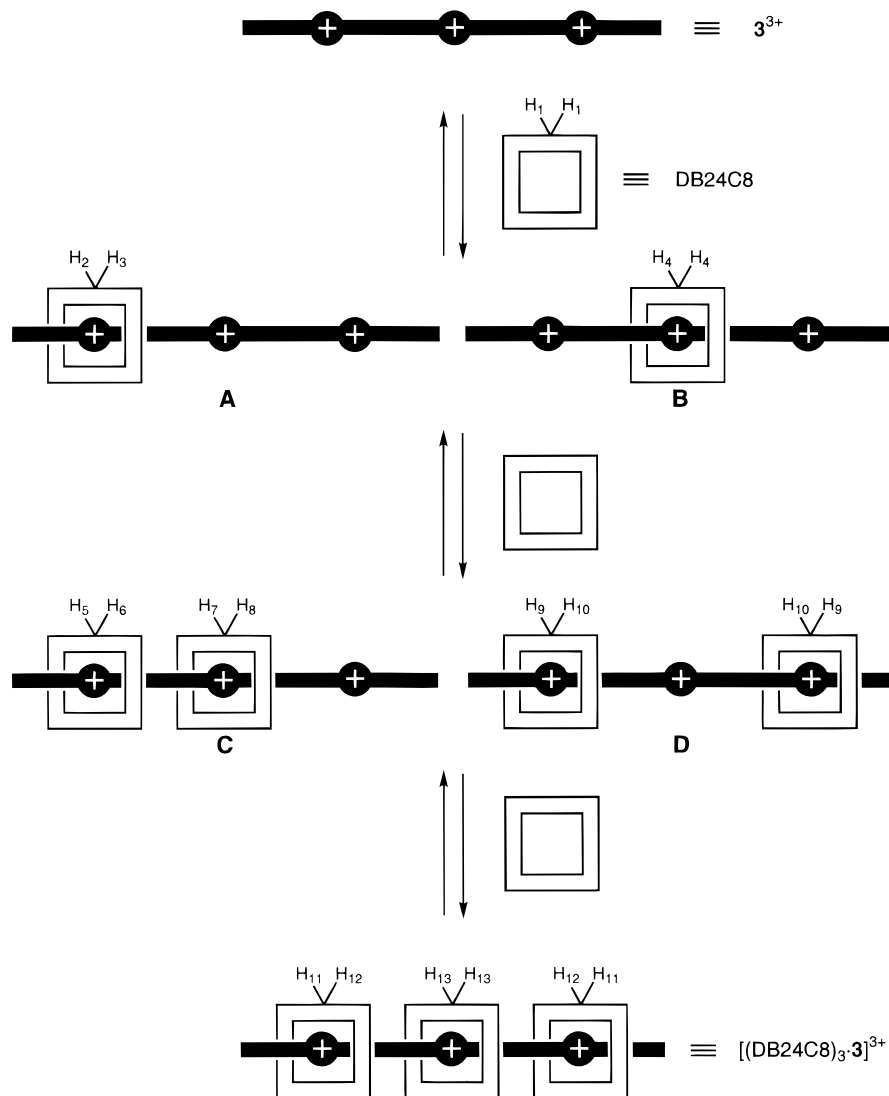
Scheme 4. Synthesis of the Tetracationic salt **4**·4PF₆

macrocycle **C**) is parallel to, and overlapping with, that of another, in a geometry which is consistent with a strong π - π stacking interaction. This interaction results in the formation of a π - π -linked [7]pseudorotaxane, the distance between the centroids of the terminal phenyl rings being 45.1 Å (*cf.*, 21.6 Å within the covalent framework of the 3³⁺ trication).²¹ Adjacent [7]pseudorotaxanes are oriented such that the catechol rings of one interleave with those of the next. Although these rings are aligned essentially parallel to each other, the interplanar distances and centroid-centroid separations are too large to represent any significant π - π interactions.

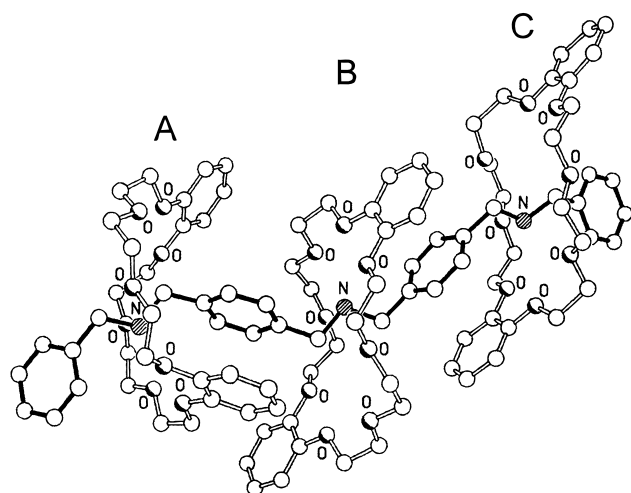
Complexation: Tetracationic Salt **4·4PF₆ and DB24C8.** Like its tricationic congener **3**·3PF₆, the tetracationic salt **4**·4PF₆ dissolves readily in MeCN and Me₂CO, but is insoluble in chlorinated solvents. However, in the presence of >4 mol equiv of DB24C8, a solution of **4**·4PF₆ in Me₂CO or MeCN may be diluted with either CHCl₃ or CH₂Cl₂ without precipitation of

the salt or its complexes, again suggesting the presence of pseudorotaxane complexes in solution. Analysis of an CD₃CN solution, containing a 4:1 molar mixture of DB24C8 and **4**·4PF₆, by ¹H NMR spectroscopy points again to the existence of a complicated mixture of uncomplexed host-guest species and a number of different complexes formed between them. For **4**·4PF₆ and DB24C8, there exists (Scheme 6) the possibility of two "isomeric" 1:1 complexes [DB24C8·**4**]⁴⁺ (**E** and **F**), four "isomeric" 2:1 complexes [(DB24C8)₂·**4**]⁴⁺ (**G**, **H**, **I**, and **J**), two "isomeric" 3:1 complexes [(DB24C8)₃·**4**]⁴⁺ (**K** and **L**), and one 4:1 complex [(DB24C8)₄·**4**]⁴⁺. Presumably, since a situation of slow kinetic exchange operates, different amounts of each of these complexes, as well as of uncomplexed **4**·4PF₆ and DB24C8, are present in solution. Not surprisingly, the spectrum is exceedingly complicated; in this case, there are 33 possible different chemical environments for the protons of each of the crown ether's α -, β -, and γ -OCH₂ groups. Nonetheless, the situation can be made less complicated by recording the spectrum of **4**·4PF₆ in the presence of an excess (~10 mol equiv) of DB24C8 in a CDCl₃/CD₃CN solvent mixture. The

(21) Further extension of this [7]pseudorotaxane does not occur: the non- π - π -stacked terminal phenyl rings are offset substantially with respect to their symmetry-related counterparts and the shortest centroid-centroid distance is 5.1 Å.

Scheme 5. Cartoon Representations Illustrating the Seven Discrete Species—Complexed and Uncomplexed—Expected for a Solution of $3 \cdot 3\text{PF}_6$ and DB24C8^a

^a Atoms labeled H₁ to H₁₃ represent the hydrogen atoms of the polyether loops' OCH₂ groups.

**Figure 3.** The 3:1 complex formed between DB24C8 and 3^{3+} in the solid state. The three independently threaded DB24C8 macrocycles are labeled A, B, and C.

¹H NMR spectrum²⁰ obtained under these conditions is remarkably simple and indicates the presence of two major species in solution, specifically, the excess of uncomplexed DB24C8 and

the [5]pseudorotaxane $[(\text{DB24C8})_4 \cdot 4]^{4+}$. Comparison of the relative intensities of the proton resonances on both the complexed tetracationic thread and complexed DB24C8 macrocycle indicate that the stoichiometry of the major complex is 4:1 (host:guest) in solution.

Repeated attempts at growing a single crystal of the 4:1 complex, suitable for X-ray crystallographic structure determination, proved fruitless. In all cases, amorphous powders were obtained from solutions of DB24C8 and $4 \cdot 4\text{PF}_6$, even after applying various techniques and solvent systems. Analysis of the powder, obtained as a result of slow evaporation of an Me₂CO solution containing a 4:1 molar ratio of DB24C8 and $4 \cdot 4\text{PF}_6$, by LSIMS revealed²⁰ an intense peak, corresponding to the [5]pseudorotaxane $[(\text{DB24C8})_4 \cdot 4 \cdot 3\text{PF}_6]^+$, at m/z 2786. Additionally, we detected peaks representing ions created as a result of the extrusion of one, two, and three DB24C8 macrocycles (with concomitant loss of HPF₆ units) from the complex. Moreover, the peak corresponding to the fully complexed thread, in this case, $[(\text{DB24C8})_4 \cdot 4 \cdot 3\text{PF}_6]^+$, exists as the peak of highest mass, with an intensity roughly 5% of that of the base peak (which in this case, is the species $[(\text{DB24C8})_4 \cdot 4 \cdot 3\text{H}]^+$). The observation of such an intense peak for a complex comprised of five components suggests that mass spectrometric soft ionization techniques are particularly valuable tools for the

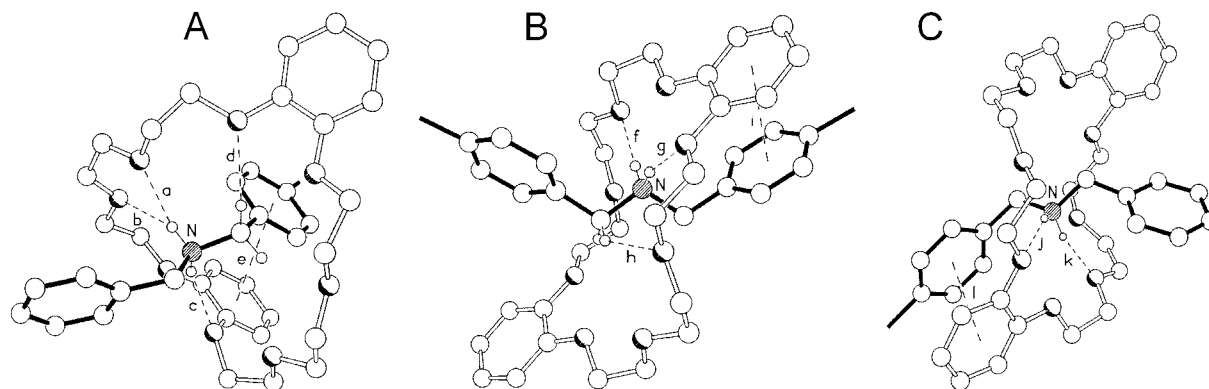


Figure 4. The host-guest hydrogen bonding and π - π stacking interactions in the $[(\text{DB24C8})_3 \cdot 3]^{3+}$ superstructure. Interactions involving macrocycle **A**: $[\text{N}^+ \cdots \text{H} \cdots \text{O}]$ hydrogen bonds $[[\text{N}^+ \cdots \text{O}], [\text{H} \cdots \text{O}]]$ distances (\AA) and $[\text{N}^+ \cdots \text{H} \cdots \text{O}]$ angles (deg) (a) 2.97, 2.18, 140; (b) 3.11, 2.28, 144; (c) 3.04, 2.15, 152; $[\text{C}-\text{H} \cdots \text{O}]$ distances and angle (d) 3.26, 2.35, 158; π - π stacking (e) interplanar separation 3.47 \AA and centroid-centroid separation 3.71 \AA . Interactions involving macrocycle **B**: $[\text{N}^+ \cdots \text{H} \cdots \text{O}]$ hydrogen bonds $[[\text{N}^+ \cdots \text{O}], [\text{H} \cdots \text{O}]]$ distances (\AA) and $[\text{N}^+ \cdots \text{H} \cdots \text{O}]$ angles (deg) (f) 2.92, 1.98, 166; (g) 3.19, 2.25, 165; $[\text{C}-\text{H} \cdots \text{O}]$ distances and angle (h) 3.28, 2.49, 140; π - π stacking (i) interplanar separation 3.47 \AA and centroid-centroid separation 3.71 \AA . Interactions involving macrocycle **C**: $[\text{N}^+ \cdots \text{H} \cdots \text{O}]$ hydrogen bonds $[[\text{N}^+ \cdots \text{O}], [\text{H} \cdots \text{O}]]$ distances (\AA) and $[\text{N}^+ \cdots \text{H} \cdots \text{O}]$ angles (deg) (j) 3.17, 2.25, 161 (k) 3.05, 2.12, 164; π - π stacking (l) interplanar separation 3.44 \AA and centroid-centroid separation 3.67 \AA .

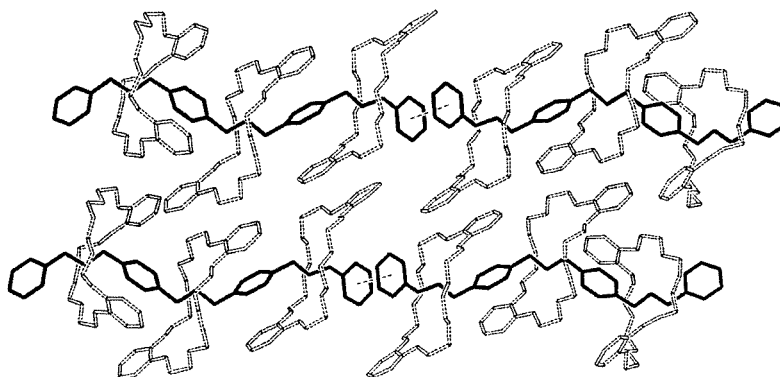


Figure 5. The packing of the [4]pseudorotaxane showing the formation of a [7]pseudorotaxane via π - π linking. The interplanar separation and centroid-centroid distance between the π -stacked trications are 3.62 and 3.66 \AA , respectively.

characterization of higher order $[n]$ pseudorotaxanes of this type in the "gas phase".

Complexation: TPP51C15 and Monocationic Salt $1 \cdot \text{PF}_6$

To explore the potential of the macrocyclic polyether TPP51C15 as a suitable host molecule for guest 1^+ ions, >3 mol equiv of $1 \cdot \text{PF}_6$ were suspended in a CDCl_3 solution of the crown ether. After filtration, the ^1H NMR spectrum obtained from the solution suggested, on the basis of the integrals associated with the signals for host and guest probe protons, that <1 equiv of the salt had been extracted into the solution. On the other hand, using CD_2Cl_2 as the extraction solvent resulted in the dissolution of what approximates very closely to 3 mol equiv of $1 \cdot \text{PF}_6$.²² Since the solubility of $1 \cdot \text{PF}_6$ in CD_2Cl_2 is extremely low in the absence of TPP51C15, we believe that all of the salt must be complexed by the crown ether in solution. Significant chemical shift changes were detected²³ for the proton resonances of both the macrocyclic polyether and 1^+ , thus indicating strong complexation between the two species in solution.

Crystals of the complex were obtained by layering a 1:3 mixture of TPP51C15 and $1 \cdot \text{PF}_6$ in CH_2Cl_2 with $n\text{-C}_6\text{H}_{14}$. Analysis of one such crystal by LSIMS failed to indicate complexation beyond a 1:2 stoichiometry. This observation was

(22) We have used this technique previously¹³ in order to determine the complexation stoichiometry for the association between BPP34C10 and $1 \cdot \text{PF}_6$ in CD_2Cl_2 .

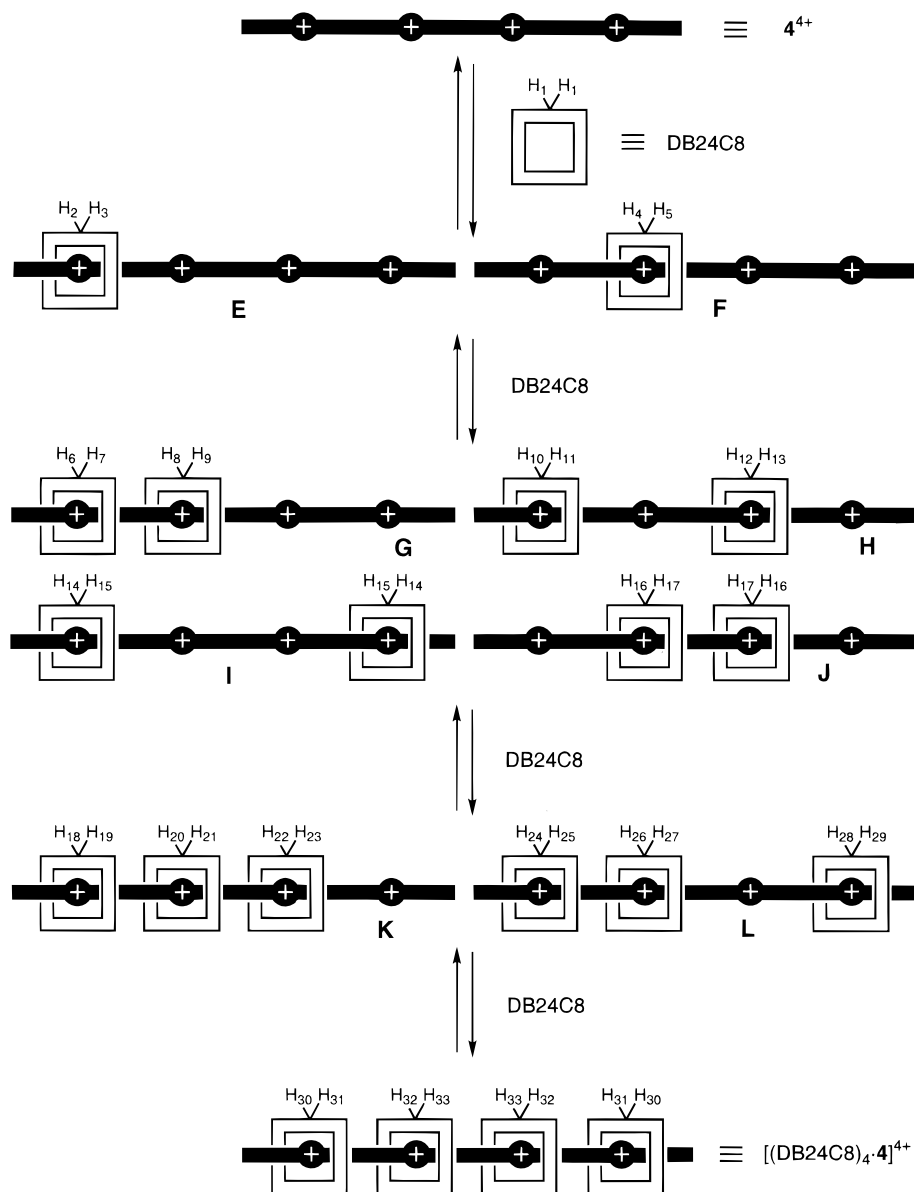
(23) $\Delta\delta$ values were obtained for the proton resonances of the polyether's α -, β -, γ -, and δ - OCH_2 and hydroquinone CH groups. For a solution of TPP51C15 ($\sim 5 \times 10^{-3}$ M) and $1 \cdot \text{PF}_6$ ($\sim 1.5 \times 10^{-2}$ M) in CD_2Cl_2 at 20 $^\circ\text{C}$ these were 0.00, -0.17, -0.29, -0.36, and +0.13 ppm, respectively.

not unexpected, since the LSI mass spectrum of a mixture of BPP34C10 and $1 \cdot \text{PF}_6$ exhibited¹³ only an extremely weak peak ($<1\%$ of the base peak's height) for a 1:2 complex. It is not unreasonable to conclude that the very large cavity of the TPP51C15 macrocycle is not suited for simultaneous accommodation of three 1^+ guest ions without a significant degree of decomplexation of at least one of them occurring in the "gas phase".

The X-ray analysis²⁴ of one of the aforementioned crystals reveals (Figure 6) a supramolecular architecture in which three 1^+ cations are threaded through the center of the TPP51C15 macrocycle, which adopts a saddlelike conformation with approximate C_s symmetry. Complex stabilization is achieved via a combination of $[\text{N}^+ \cdots \text{H} \cdots \text{O}]$ and $[\text{C}-\text{H} \cdots \text{O}]$ hydrogen bonding. Despite the large number of aromatic rings in the 1:3 complex, there is a marked absence of any intra- or intercomplex face-to-face or edge-to-face interactions. The packing interactions appear to be only of a van der Waals nature. However, inspection of the relationship between the cations and anions reveals that one of the PF_6^- anions is located almost centrally within the cleft formed by the folded saddlelike co-conformation²⁵ of the 1:3 complex (Figure 6). The planes of the three hydroquinone rings, together with one of the phenyl

(24) Fyfe, M. C. T.; Glink, P. T.; Menzer, S.; Stoddart, J. F.; White, A. J. P.; Williams, D. J. *Angew. Chem., Int. Ed. Engl.* **1997**, *36*, 2068-2070.

(25) Strictly speaking, the term "conformation" refers only to discrete molecular species. Consequently, we have used²⁴ "co-conformation" to designate the three-dimensional spatial arrangement of the atoms in supramolecular systems.

Scheme 6. Cartoon Representations of the 11 Discrete Species—Complexed and Uncomplexed—Expected for a Solution Containing a Mixture of $4\cdot 4\text{PF}_6$ and DB24C8^a

^a Atoms labeled H₁ to H₃₃ represent the hydrogen atoms of the polyether loops' OCH₂ groups.

rings of one of the 1^+ cations, are all inclined toward, and intersect at, the phosphorus atom. An analysis of [C—H...F] contacts reveals the presence of several stabilizing hydrogen bonding interactions with [H...F] distances in the range 2.43–2.67 Å (associated [C...F] distances range from 3.20–3.51 Å). It is interesting to note that hydrogen atoms of both hydroquinone rings and benzylic methylene groups are involved in these interactions.

Complexation: TPP68C20 and Monocationic Salt $1\cdot\text{PF}_6$. Deployment of the macrocyclic polyether TPP68C20, which possesses four polyether loops each capable, in principle, of binding secondary dialkylammonium ions, provided some notable findings in its complexation behavior with $1\cdot\text{PF}_6$. In order to obtain information on the complex's approximate stoichiometry, we used the established technique (*vide supra*) of extracting this insoluble salt into a TPP68C20-containing CD₂Cl₂ solution. Using this technique, we observed, by ¹H NMR spectroscopy,²⁰ the dissolution of an amount of salt that approximates to the extraction of 4 mol equiv of $1\cdot\text{PF}_6$ from a CD₂Cl₂ suspension containing about a 10-fold excess of the salt. Once again, significant chemical shift changes were observed²⁶

for the proton resonances on both the host and guest species, suggesting strong intercomponent association in CD₂Cl₂.

Analysis of a 1:4 mixture of TPP68C20 and $1\cdot\text{PF}_6$ by LSIMS did not reveal any host–guest association beyond a 1:2 stoichiometry. This result is entirely in line with that observed for the “gas phase” association of the [TPP51C15·(1)₃][3PF₆] system. It suggests that, for the most part, it is not possible to obtain meaningful information (*i.e.*, observing peaks corresponding to “fully” complexed supramolecular entities) on the “gas phase” association between secondary dialkylammonium ions and these very large ring crown ethers using this particular soft ionization technique.

A suitable single crystal for X-ray crystallography was grown by liquid diffusion of *n*-C₆H₁₄ into a CH₂Cl₂ solution containing a 1:4 molar mixture of TPP68C20 and $1\cdot\text{PF}_6$. The X-ray analysis of one of these crystals reveals²⁴ the creation of a crystalline aggregate containing two independent 1:4 complexes

(26) $\Delta\delta$ values were obtained for the proton resonances of the polyether's α -, β -, γ -, and δ -OCH₂ and hydroquinone CH groups. For a solution of TPP68C20 ($\sim 5 \times 10^{-3}$ M) and $1\cdot\text{PF}_6$ ($\sim 2.0 \times 10^{-2}$ M) in CD₂Cl₂ at 20 °C these were –0.03, –0.15, –0.23, –0.38, and +0.16 ppm, respectively.

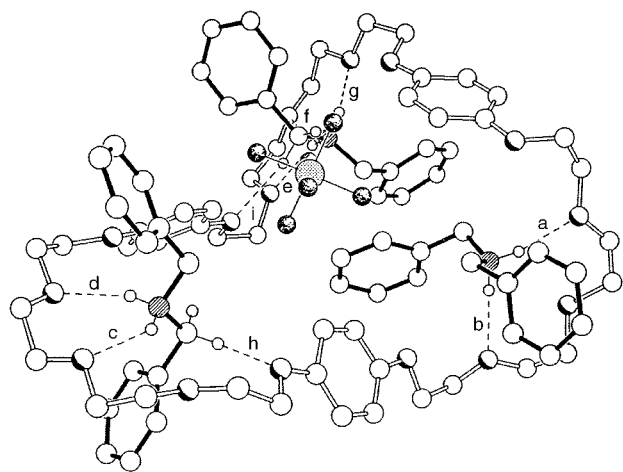


Figure 6. Ball-and-stick representation of the 1:3 complex [TPP51C15-(1)₃]³⁺ in the solid state, showing the [N⁺—H···O] and [C—H···O] hydrogen-bonding interactions and the PF₆[−] anion that interacts with the supermolecule. [N⁺—H···O] hydrogen bonds [[N⁺···O], [H···O] distances (Å), [N⁺—H···O] angles (deg)]: (a) 2.89, 1.94, 168; (b) 3.02, 2.07, 176; (c) 2.88, 2.09, 138; (d) 2.91, 2.02, 153; (e) 2.98, 2.16, 142; (f) 2.86, 2.09, 137; (g) 2.85, 1.95, 155; [C—H···O] distances and angles (h) 3.36, 2.47, 155; (i) 3.38, 2.45, 163.

(Figure 7), together with an additional pair of nonrelated C_s symmetric 1⁺ cations, all with their associated PF₆[−] counterions, in the asymmetric unit. The two 1:4 complexes have essentially identical geometries with each TPP68C20 macrocycle adopting a tennis ball seam-like conformation with S₄ symmetry. Complex stabilization is achieved via a combination of [N⁺—H···O] and [C—H···O] hydrogen-bonding interactions between the hydrogen atoms of the ammonium centers, and their adjacent CH₂ groups, with oxygen atoms from the macrocyclic polyether. The nonthreaded cations, which lie on the crystallographic C_s plane, are not involved in any hydrogen-bonding interactions. The only notable intercomplex interaction is an aromatic—aromatic edge-to-face association between one of the phenyl rings of a 1⁺ ion in one complex and one of the macrocyclic polyether's hydroquinone rings in the other (the [H···π] distance is 2.75 Å and the associated [C—H···π] angle is 138°). The most striking feature of the 1:4 complexes is the siting (Figure 7) of a single PF₆[−] anion within their cores in an ordered arrangement. The anion is totally encapsulated by both the four hydroquinone rings, which are oriented with their planes intersecting on the phosphorus center, and the four tetrahedrally disposed, positively charged CH₂—NH₂⁺—CH₂ units of the four 1⁺ cations (Figure 8). The phosphorus atoms lie only ~0.3 Å from the complexes' centroids. As in the 1:3 complex (*vide supra*), the anion is held in place by [C—H···F] hydrogen bonds involving a combination of hydroquinone methine and benzylic methylene hydrogen atoms. The [H···F] distances range between 2.41–2.73 Å, with associated [C···F] contacts of between 3.16–3.52 Å.

Conclusions

The research documented in this Article represents a significant extension (Figure 9) to the knowledge that we have already obtained from studying relatively simple host—guest systems based upon interactions between macrocyclic polyether hosts and secondary dialkylammonium ion guests. By either extending the number of recognition sites in the threadlike oligocations, or by increasing the size of the crown ether macrorings, we have demonstrated that the control and predictability of the binding modes, in addition to the complexation stoichiometries of the resulting solution- and solid-state superstructures (and

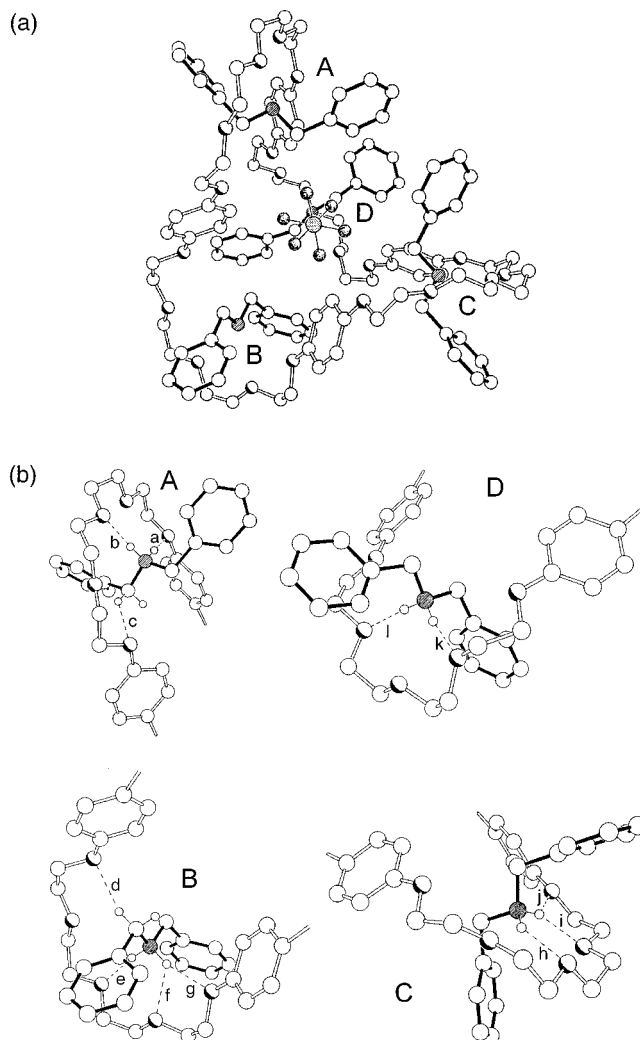


Figure 7. (a) Ball-and-stick representation of the solid-state superstructure of one of the 1:4 complexes [TPP68C20-(1)₄]⁴⁺, illustrating the gross binding mode of the threadlike cations by the macrocyclic polyether that permits the complete encapsulation of a PF₆[−] anion. (b) Detailed analysis of the [N⁺—H···O] and [C—H···O] hydrogen-bonding interactions for the four independent complexation sites (A–D). [X—H···O] Hydrogen bonds [[X···O], [H···O] distances (Å), [X—H···O] angles (deg)]: (a) 3.00, 2.04, 170; (b) 3.01, 2.05, 174; (c) 3.24, 2.35, 154; (d) 3.29, 2.40, 155; (e) 2.87, 1.92, 171; (f) 2.86, 2.25, 120; (g) 3.07, 2.15, 160; (h) 2.78, 1.88, 155; (i) 2.98, 2.25, 132; (j) 3.20, 2.33, 151; (k) 2.91, 1.96, 170; (l) 2.82, 1.89, 162. The other 1:4 complex exhibits a virtually identical hydrogen-bonding array. [X—H···O] hydrogen bonds [[X···O], [H···O] distances (Å), [X—H···O] angles (deg)]: (a) 2.98, 2.03, 168; (b) 2.95, 2.00, 170; (c) 3.26, 2.45, 141; (d) 3.33, 2.41, 161; (e) 2.88, 1.92, 172; (f) 2.87, 2.28, 119; (g) 3.10, 2.17, 162; (h) 2.89, 2.08, 141; (i) 2.85, 2.00, 148; (j) 3.19, 2.46, 133; (k) 2.93, 1.97, 177; (l) 2.83, 1.88, 169.

in some cases, the “gas phase”), is retained, although with occasional surprises. Nonetheless, these self-assembling systems are characterized by their simplicity on the one hand (*i.e.*, constitutionally), and their complexity and intricacy (*i.e.*, superstructurally) on the other.

Experimental Section

General. Anhydrous THF and MeCN were distilled from sodium benzophenone ketyl and CaH₂, respectively. Column chromatography was carried out using silica gel 60F (Merck 9385, 230–400 mesh). Melting points were determined on an Electrothermal 9200 apparatus and are uncorrected. ¹H NMR spectra were recorded on either a Bruker AC300 (300.1 MHz) spectrometer or a Bruker AMX400 (400.1 MHz) spectrometer at 20 °C using either the solvent reference or TMS as the

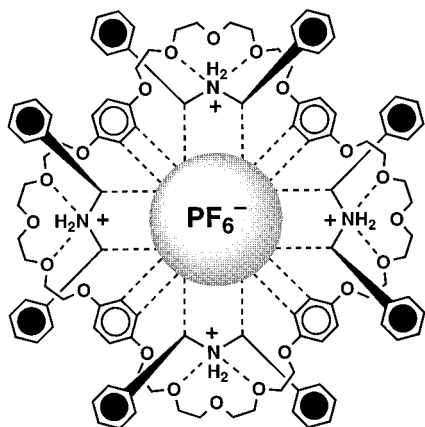


Figure 8. Cartoon representation depicting the binding of one of the PF₆⁻ anions within the cavity formed by one of the 1:4 complexes [TPP68C20·(1)₄]⁴⁺.

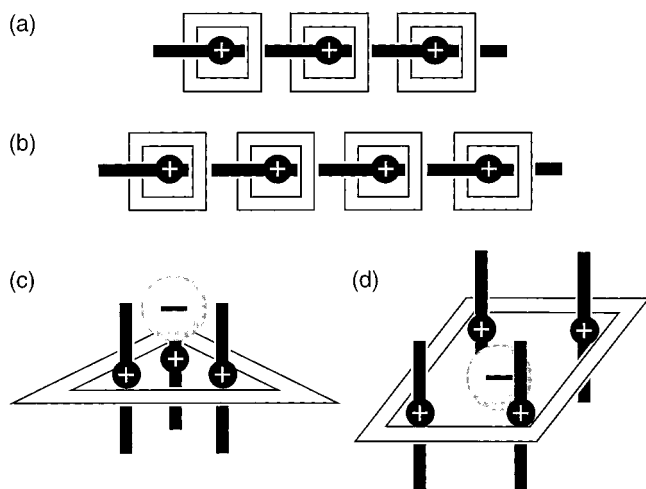


Figure 9. Cartoons representing the pseudorotaxane superstructures which have been described in this Article: (a) a triply encircled [4]pseudorotaxane; (b) a quadruply encircled [5]pseudorotaxane; (c) a triply stranded [4]pseudorotaxane which partially envelops an anion; and (d) a quadruply stranded [5]pseudorotaxane which totally encapsulates an anion.

internal standard. ¹³C NMR spectra were recorded on a Bruker AC300 (75.5 MHz) spectrometer or a Bruker AMX400 (100.6 MHz) spectrometer at 20 °C. Liquid secondary ion mass spectra (LSIMS) were obtained from a VG Zabspec mass spectrometer, using either a *m*-nitrobenzyl alcohol or a thioglycerol matrix, operating in the positive ion mode at a scan speed of 5 s per decade. Microanalyses were performed by the Microanalysis Department at the University of North London.

***N*-(*tert*-Butoxycarbonyl)bis(4-formylbenzyl)amine (6).** PCC (420 mg, 1.95 mmol) was added to a solution of *N*-(*tert*-butoxycarbonyl)-bis[4-(hydroxymethyl)benzyl]amine¹⁴ (**5**) (348 mg, 0.97 mmol) in CH₂Cl₂ (25 mL), and the resulting solution was stirred under a N₂ atmosphere for 2 h. The mixture was then washed with H₂O (50 mL), and the aqueous phase was extracted with CH₂Cl₂ (3 × 50 mL). The combined organic phases were then dried (MgSO₄), the solvent was evaporated under reduced pressure, and the residue subjected to column chromatography (EtOAc/*n*-C₆H₁₄, 1:2) to yield the bisaldehyde **6** as a colorless, viscous oil (311 mg, 91%): ¹H NMR (CDCl₃) δ 1.48 (9H, s), 4.45 and 4.53 (both 2H, two br), 7.36 (4H, br s), 7.86 (4H, d, *J* = 8 Hz), 10.02 (2H, s); ¹³C NMR (CDCl₃) δ 28.3, 49.9 (br), 80.9, 127.6 and 128.2 (both br), 130.1, 135.7, 144.8, 155.7, 191.7; LSIMS *m/z* (%) 354 (32) [M + H]⁺, 298 (100) [M + H - C₄H₈]⁺. Anal. Calcd for C₂₁H₂₃NO₄: C, 71.37; H, 6.56; N, 3.96. Found: C, 71.31; H, 6.41; N, 3.99.

Tricationic Salt 3·3PF₆. The bisaldehyde **6** (186 mg, 0.55 mmol) and benzylamine (148 mg, 1.38 mmol) were dissolved in PhMe (50 mL), and the solvent was evaporated *in vacuo* at ~60 °C. The residue

was dissolved in PhMe (50 mL), and the solvent was evaporated again. This procedure was repeated twice to yield a thick oil [¹H NMR (CDCl₃) δ 1.52 (9H, br), 4.39 and 4.50 (both 2H, two br), 4.85 (4H, s), 7.10–7.40 (14H, m), 7.76 (4H, d, *J* = 8 Hz), 8.42 (2H, s)] which was dissolved in MeOH (50 mL). NaBH₄ (1.0 g, excess) was added with stirring portionwise to the solution over a period of 60 min, and then the reaction mixture was quenched by the addition of 2 N HCl to adjust the pH to less than 2. The solvents were evaporated *in vacuo*, and the residue was partitioned between CHCl₃ (50 mL) and a 10% NaOH solution (50 mL). The aqueous phase was further extracted with CHCl₃ (3 × 50 mL). The combined organic phases were dried (MgSO₄), and the solvent was evaporated to yield a thick oil [¹H NMR (CDCl₃) δ 1.48 (9H, s), 1.70 (2H, br), 3.80 (4H, s), 3.83 (4H, s), 4.33 and 4.40 (both 2H, two br), 7.18 (4H, br), 7.23–7.40 (14H, m)] which was dissolved in CH₂Cl₂ (50 mL). TFA (1 mL, excess) was added, and the solution was stirred for 12 h. The solution was washed with a 10% NaOH solution (50 mL) and dried (MgSO₄), and the solvent was evaporated to yield a thick oil. HCl (2 N, 50 mL) was added, and the mixture was sonicated to break up the resulting solid. The HCl solution was evaporated under reduced pressure, and the residue was suspended in Me₂CO (10 mL). A solution of NH₄PF₆ (1.0 g, excess) in H₂O (2 mL) was added. After more H₂O had been added to the suspension to effect dissolution, the mixture was filtered to remove insoluble materials. Ultimately, a copious amount of H₂O was added to the filtrate, causing a precipitate to form, which was collected, washed with cold H₂O (3 × 5 mL), and dried to yield the tetracationic salt **3·3PF₆** (187 mg, 39%) as an off-white solid: ¹H NMR (CD₃CN) δ 4.25–4.35 (12H, m), 7.20 (6H, br), 7.48 (10H, s), 7.56 (8H, s); ¹³C NMR (CDCl₃) δ 51.7, 51.9, 52.5, 130.0, 130.7, 131.1, 131.2, 131.7, 132.1, 132.6, 132.8; LSIMS *m/z* (%) 582 (12) [M - PF₆ - HPF₆]⁺, 436 (100) [M - PF₆ - 2HPF₆]⁺. Anal. Calcd for C₃₀H₃₆N₃P₃F₁₈: C, 41.25; H, 4.15; N, 4.81. Found: C, 41.25; H, 4.16; N, 4.96.

***N*-(*tert*-Butoxycarbonyl)-*N*-benzyl-4-carbomethoxybenzylamine (7).** Benzylamine (1.38 g, 12.9 mmol) and methyl 4-formylbenzoate (2.11 g, 12.9 mmol) were condensed in PhMe (200 mL), using a similar procedure to that described above (*vide* preparation of **3·3PF₆**), to furnish a thick oil [¹H NMR (CDCl₃) δ 3.95 (3H, s), 4.87 (2H, s), 7.24–7.45 (5H, m), 7.85 (2H, d, *J* = 8 Hz), 8.09 (2H, d, *J* = 8 Hz), 8.45 (1H, s)], which was reduced with NaBH₄ (*vide* preparation of **3·3PF₆**). The oily product was dissolved in CH₂Cl₂ (100 mL). Boc₂O (2.82 g, 12.9 mmol) and DMAP (20 mg, 0.16 mmol) were added, and the resulting solution was stirred at ambient temperature for 12 h. The solvent was evaporated to yield a colorless oil (4.45 g, 97%), a small portion of which was purified by column chromatography (EtOAc/*n*-C₆H₁₄, 1:4) for analytical purposes which was characterized as the title compound **7**: ¹H NMR (CDCl₃) δ 1.47 (9H, br), 3.92 (3H, s), 4.36 and 4.48 (both 2H, two br), 7.10–7.36 (7H, m), 8.00 (2H, d, *J* = 8 Hz); ¹³C NMR (CDCl₃) δ 28.3, 48.9/49.3/49.6 (three br), 52.0, 80.3, 127.0/127.3 (two br), 127.7/127.9 (two br), 128.5, 129.0, 129.8, 137.6, 139.9, 143.4, 155.9, 166.8; LSIMS *m/z* (%) 356 (8) [M + H]⁺, 300 (100) [M + H - C₄H₈]⁺. Anal. Calcd for C₂₁H₂₅NO₄: C, 70.96; H, 7.09; N, 3.94. Found: C, 71.09; H, 6.99; N, 4.07.

***N*-(*tert*-Butoxycarbonyl)-*N*-benzyl-4-(hydroxymethyl)benzylamine (8).** A solution of the ester **7** (4.40 g, 12.4 mmol) in THF (250 mL) was heated under reflux and then cooled. LiAlH₄ (2.0 g, 52.7 mmol) was added portionwise to the warm solution over 30 min. The reaction mixture was then heated under reflux for 12 h, before being cooled down to ambient temperature. H₂O was added until the remaining aluminum hydrides had been quenched and then 2 N HCl was added until the pH was less than 2. The solvents were evaporated, and the residue was partitioned between H₂O (100 mL) and CH₂Cl₂ (100 mL), with the aqueous phase being extracted further with CH₂Cl₂ (3 × 100 mL). The combined extracts were dried (MgSO₄). The solvent was then evaporated off to yield a clear oil (3.52 g, 87%), a small portion of which was purified by column chromatography (EtOAc/*n*-C₆H₁₄, 2:3) to afford the title compound **8**: ¹H NMR (CDCl₃) δ 1.49 (9H, s), 1.90 (1H, br), 4.33 and 4.40 (both 2H, two br), 4.67 (2H, s), 7.14–7.23 (4H, br), 7.23–7.40 (5H, m); ¹³C NMR (CDCl₃) δ 28.4, 48.9, 65.1, 80.1, 127.2, 127.9, 128.2, 128.5, 129.1, 137.4, 137.9, 139.9, 156.0, 191.7; LSIMS *m/z* (%) 328 (18) [M + H]⁺, 272 (100) [M + H - C₄H₈]⁺. Anal. Calcd for C₂₀H₂₅NO₃: C, 73.37; H, 7.70; N, 4.28. Found: C, 73.54; H, 7.82; N, 3.98.

Table 1. Crystal Data, Data Collection, and Refinement Parameters^a

	[(DB24C8) ₃ ·3][PF ₆] ₃	[TPP51C15·(1) ₃][PF ₆] ₃	[TPP68C20·(1) ₄][PF ₆] ₄
formula	C ₁₀₂ H ₁₃₂ N ₃ O ₂₄ ·3PF ₆	C ₈₄ H ₁₀₈ N ₃ O ₁₅ ·3PF ₆	C ₁₁₂ H ₁₄₄ N ₄ O ₂₀ ·4PF ₆ · [0.5(C ₆ H ₅ CH ₂) ₂ NH ₂ ·0.5PF ₆]
solvent	Me ₂ CO·0.25H ₂ O	2CH ₂ Cl ₂	1.75CH ₂ Cl ₂
formula weight	2281.6	2004.5	2766.4
color, habit	red plates	colorless blocks	colorless blocks
crystal size, mm	0.60 × 0.23 × 0.13	0.67 × 0.43 × 0.20	0.77 × 0.66 × 0.60
lattice type	triclinic	orthorhombic	monoclinic
space group	<i>P</i> 1̄	<i>Pca</i> 2 ₁	<i>P</i> 2 ₁ / <i>m</i>
<i>T</i> , K	218	293	173
cell dimensions			
<i>a</i> , Å	11.909(5)	19.592(1)	19.179(3)
<i>b</i> , Å	14.926(5)	25.240(1)	70.669(7)
<i>c</i> , Å	36.100(5)	20.117(3)	19.993(2)
<i>α</i> , deg	87.87(1)		
<i>β</i> , deg	83.45(1)		90.55(1)
<i>γ</i> , deg	68.28(1)		
<i>V</i> , Å ³	5922(3)	9948(2)	27096(6)
<i>Z</i>	2	4	8 ^b
<i>D_c</i> , g cm ⁻³	1.279	1.338	1.356
<i>F</i> (000)	2397	4176	11532
<i>μ</i> , mm ⁻¹	1.294	2.350	2.083
<i>θ</i> range, deg	1.2–50.0	1.8–60.0	1.3–55.0
no. of unique reflections: measured	12155	6518	34335
observed, <i>F</i> ₀ > 4σ(<i>F</i> ₀)	6760	3846	20274
no. of variables	1211	670	3282
<i>R</i> ₁ ^c	0.134	0.103	0.100
<i>wR</i> ₂ ^d	0.359	0.269	0.269
weighting factors	0.274, 6.568	0.175, 18.974	0.199, 41.458
<i>a</i> , <i>b</i> ^e			
largest difference peak, hole, eÅ ⁻³	1.11, -0.66	0.39, -0.33	1.42, -0.82

^a Details in common: graphite monochromated Cu Kα radiation, ω scans, Siemens P4 rotating anode diffractometer, refinement based on *F*².

^b There are two crystallographically independent molecules in the asymmetric unit. ^c *R*₁ = Σ||*F*_o| - |*F*_c||/Σ|*F*_o|. ^d *wR*₂ = √{Σ[w(*F*_o² - *F*_c²)²]/Σ[w(*F*_o²)²]}. ^e *w*⁻¹ = σ²(*F*_o²) + (*aP*)² + *bP*.

***N*-(*tert*-Butoxycarbonyl)-*N*-benzyl-4-formylbenzylamine (9).** A solution of the alcohol **8** (1.0 g, 3.05 mmol) in CH₂Cl₂ (10 mL) was added portionwise to a suspension of PCC (0.66 g, 3.05 mmol) in CH₂Cl₂ (70 mL), and the reaction mixture stirred vigorously at ambient temperature. Further quantities of PCC (a total of 0.50 g, 2.32 mmol) were added portionwise over the next 45 min. The solution was then washed with 1 N NaOH (4 × 100 mL) until no color remained in the organic phase, which was then dried (MgSO₄). The solvent was evaporated to yield a white solid (0.80 g, 81%), a portion of which was subjected to column chromatography (EtOAc/*n*-C₆H₁₄, 1:4) to obtain a significantly purer sample of the title compound **9**: ¹H NMR (CDCl₃) δ 1.50 (9H, s), 4.40 and 4.48 (both 2H, two br), 7.12–7.48 (7H, m), 7.85 (2H, d, *J* = 8 Hz), 9.98 (1H, s); ¹³C NMR (CDCl₃) δ 28.4, 44.9 and 49.9 (both br), 80.5, 127.4, 128.0 (br), 128.6, 130.0, 131.2, 135.5, 137.5, 150.0 (br), 155.9, 191.8; LSIMS *m/z* (%) 326 (15) [M + H]⁺, 270 (100) [M + H - C₄H₈]⁺. Anal. Calcd for C₂₀H₂₃N₃O₃: C, 73.82; H, 7.12; N, 4.30. Found: C, 73.71; H, 7.15; N, 4.43.

Tetracationic Salt 4·4PF₆. The aldehyde **9** (0.80 g, 2.46 mmol) and *p*-xylylenediamine (0.187g, 1.37 mmol) were condensed in PhMe (200 mL), using a procedure similar to one described above (*vide* preparation of 3·3PF₆), to provide a thick, pale yellow oil [¹H NMR (CDCl₃) δ 1.52 (18H, br s), 4.38 and 4.46 (8H, br m), 4.83 (4H, s), 7.15–7.42 (18H, m), 7.75 (4H, d, *J* = 8 Hz), 8.38 (2H, br s)] which was reduced with NaBH₄ (*vide* preparation of 3·3PF₆) to yield a thick oil [¹H NMR (CDCl₃) δ 1.52 (18H, br s), 3.82 (8H, br s), 4.34 and 4.43 (both 4H, two br), 7.10–7.24 (8H, br), 7.24–7.40 (14H, m)] that was converted into the tetracationic salt 4·4PF₆ (0.81 g, 58%), using a similar procedure to that delineated for 3·3PF₆, which was isolated as a white, amorphous solid: ¹H NMR (CD₃CN) δ 4.27 (4H, s), 4.29 (4H, s), 4.31 (8H, s), 7.00 (8H, br), 7.48 (10H, s), 7.56 (8H, s), 7.57 (4H, s); ¹³C NMR (CDCl₃) δ 51.7, 52.0, 52.6, 130.0, 130.8, 131.1, 131.7 (m), 132.8 (m); LSIMS *m/z* (%) 701 (8) [M - PF₆ - HPF₆]⁺, 555 (100) [M - PF₆ - 2HPF₆]⁺. Anal. Calcd for C₃₈H₄₆N₄P₄F₂₄: C, 40.08; H, 4.07; N, 4.92. Found: C, 40.18; H, 4.13; N, 5.02.

X-ray Crystallography. Table 1 provides a summary of the crystal data, data collection and refinement parameters for the [(DB24C8)₃·3][PF₆]₃, [TPP51C15·(1)₃][PF₆]₃, and [TPP68C20·(1)₄][PF₆]₄ complexes.

All the structures were solved by direct methods and were refined by full-matrix least squares based on *F*² (blocked in the case of [TPP68C20·(1)₄][PF₆]₄). In structure [(DB24C8)₃·3][PF₆]₃, part of one of the crown ethers was found to be disordered. This disorder was resolved into two alternate, 50% occupancy orientations which were refined isotropically. The rest of the complex in this structure, and the whole of the complexes in the other two structures, were ordered and of full occupancy. In [(DB24C8)₃·3][PF₆]₃ and [TPP68C20·(1)₄][PF₆]₄, all of these atoms were refined anisotropically, but in [TPP51C15·(1)₃][PF₆]₃, only the oxygen and nitrogen atoms of the complex were refined anisotropically, the carbon atoms being treated isotropically. Each of the structures contain PF₆⁻ anions; in [(DB24C8)₃·3][PF₆]₃ and [TPP51C15·(1)₃][PF₆]₃ these anions were ordered and refined anisotropically, but in [TPP68C20·(1)₄][PF₆]₄ there were a mixture of ordered and disordered PF₆⁻ anions, the latter distributed over multiple partial occupancy sites. Only the major occupancy atoms were refined anisotropically. The nonthreading 1⁺ ions in [TPP68C20·(1)₄][PF₆]₄ were found to have crystallographic C_s symmetry and were refined anisotropically. All three structures included solvent molecules; in [TPP68C20·(1)₄][PF₆]₄ the CH₂Cl₂ molecules were ordered, of full and partial occupancy, and were refined anisotropically. The full occupancy Me₂CO molecule in [(DB24C8)₃·3][PF₆]₃ was refined anisotropically, but the 25% occupancy H₂O molecule was refined isotropically. In [TPP51C15·(1)₃][PF₆]₃, only the chlorine atoms of the disordered, partial occupancy CH₂Cl₂ molecules were refined anisotropically. All of the C–H hydrogen atoms in each of the three structures were placed in calculated positions, were assigned isotropic thermal parameters, *U*(H) = 1.2*U*_{eq}(C) [*U*(H) = 1.5*U*_{eq}(C–Me)], and were allowed to ride on their parent atoms. In all three structures, the N–H hydrogen atoms were located from Δ*F* maps and were subsequently optimized, were assigned isotropic thermal parameters, *U*(H) = 1.2*U*_{eq}(N), and were allowed to ride on their parent atoms. The hydrogen atoms of the partial occupancy H₂O molecule in [(DB24C8)₃·3][PF₆]₃ were not located. Complex [TPP51C15·(1)₃][PF₆]₃ crystallized in a polar space group (*Pca*2₁); the polarity of the structure was determined using the Flack

parameter [$x^+ = 0.20(15)$, $x^- = 0.80(15)$]. Computations were carried out using the SHELXTL PC program system.²⁷

Acknowledgment. This research, which was funded in the UK by the ZENECA Strategic Research Fund, was also supported additionally by the Biotechnology and Biological Sciences Research Council and the Engineering and Physical Sciences Research Council. We thank Dr. Ewan Chrystal

(27) SHELXTL PC version 5.03, Siemens Analytical X-Ray Instruments, Inc., Madison, WI, 1994.

(ZENECA Agrochemicals) and Drs. Peter Tasker and Andrew Collins (ZENECA Specialities) for fruitful discussions.

Supporting Information Available: Crystallographic data for [(DB24C8)₃·3][PF₆]₃ in addition to LSI mass and ¹H NMR spectra (19 pages). See any current masthead page for ordering and Internet access instructions.

JA9714806